Astrometric observations of Phobos and Deimos during solar transits imaged by the Curiosity Mastcam. M. T. Lemmon[1], J.F. Bell III[2], M.C. Malin[3], K.M. Bean[1], M.J. Wolff[4], A. Vasavada[5], F.J. Martín-Torres[6], M.-P. Zorzano-Mier[6], and the MSL Science Team. [1]Texas A&M University, College Station, TX, USA, [2]Arizona State University, Phoenix, AZ, USA; [3]Malin Space Science Systems, San Diego, CA, USA; [4]Space Science Institute, Boulder, CO, USA; [5]Jet Propulsion Laboratory, Pasadena, CA, USA; [5]Centro de Astrobiología, Madrid, Spain.

Introduction: Precise observations of the positions of the Martian moons can be used to refine knowledge of their orbits, allowing measurement of the rate at which their orbits evolve [1,2,3]. Orbital evolution probes Mars' interior elasticity, as Phobos is slowed by the tidal bulge it raises on Mars, causing its orbit to decay [2,3]. Observations of solar transits of Phobos and Deimos provide precise positional knowledge relative to a well-known reference [1]. Such transits have been predicted at the Mars Science Laboratory (MSL) field site using current ephemerides [4].

Observations: Three transit events were targeted with the MSL Mastcam. Mastcam comprises two cameras with 34-mm and 100-mm focal lengths. Each is equipped with a solar filter to allow well-exposed Sun images, and is capable of taking images in video mode. The instantaneous field of view for the cameras is 220 and 74 μrad, respectively, yielding typical solar apparent diameters of ~26 and ~80 pixels.

Observations were designed to take a large number of video frames with each camera, with moderate subframes around the expected location of the Sun (they are further cropped for presentation below). Constraints that affected observation design include small uncertainties in attitude knowledge; uncertainty in time from sequence activation to initiation of video mode; and constraints imposed by the fact that Mastcam is co-aligned with ChemCam, which can be damaged by the Sun shining in its optics improperly. The observation created a large number of video frames (see table 1) returned as thumbnail images; these were inspected and the interesting subset were selected for downlink. Key images were returned with lossless compression, and the video was completed with high-quality JPEG compressed images.

Table 1. Observation details.

Sol	37	42	42
Moon	Phobos	Phobos	Deimos
T_{REF}, s	400785169	401195801	401219643
Date, UTC	9/13/12	9/17/12	9/18/12
Time, UTC	5:15:30.2	23:19:26.0	5:56:48.3
Frames	384, 256	240, 240	464, 720
Images	55, 43	19, 19	175,153
Frames/s	2.92, 2.13	0.49, 0.46	1.48, 1.30
Δt, s	-0.3	0.4	-3.0
Δp, deg	-0.0283	0.0209	0.0047
Δx, km	-0.15	0.25	4.47
Δy, km	3.43	3.14	1.65

Table 1 provides observation details. T_{REF} is a reference time (T_{REF}) near the center of the transit in spacecraft clock (SCLK). That time is also given using current best conversion in UTC *date* and *time*. The numbers of video *frames* taken and transit-related full *images* downlinked are given for the M-34 and M-100, respectively, as is the frame rate (*frames/s)*. The remaining rows are discussed below.

Sol 37, Phobos. First was a Phobos transit on sol (Martian solar day) 37, in the mid-afternoon. It was a grazing transit in the West at 41° elevation, with Phobos rising slightly to the Sun's south over ~16 s.

Sol 42, Phobos. The second event was just after sunrise on sol 42, with Phobos setting in the East, north of the Sun. The event was a partial, rather than annular, eclipse. Due to the low elevation and high atmospheric dust load, 0.9-s exposures were used (rather than 45 ms) with the knowledge that signal would still be lower than ideal. Figure 1 shows images taken near the center of the transit; most of the granularity is image noise, but sunspots are visible. Solar limb darkening and a vertical variation in dust extinction due to varying airmass are both apparent. The duration was ~30 s.

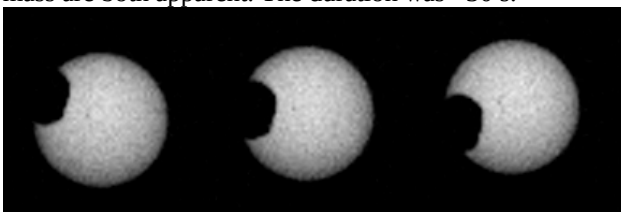

Fig. 1. Three M-100 images of Sol 42 Phobos transit.

Sol 42, Deimos. The third event was later on sol 42, and was the slowest. Deimos' apparent motion is in the same direction as the Sun (Phobos moves oppositely). The event was to the Northwest at an elevation of 77°. Deimos passed to the Sun's north, with all 4 transit contacts observed over ~114 s.

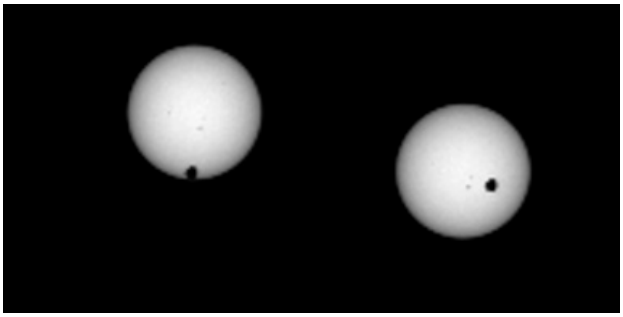

Fig. 2. Deimos transit with M-100, near second contact and event center. Sunspots are visible.

Analysis: The astrometric measurements require the angular position of the satellite with respect to the Sun, and the time at which it is at that position. Due to the short durations, the satellite motion relative to the Sun is linear. The expected perturbations from the known orbits are small. We use two numbers to describe the measurements: the time and distance of closest approach. No other statistically significant information is likely to be available.

The first challenge was to place the images in sequential order. Time tags in the data products associated with the image acquisition time are given in spacecraft clock (SCLK), which counts seconds; the sub-SCLK, which counts fractional seconds, is omitted (although it is present for product creation time). The frame rate was almost 3/s in the best case, rendering SCLK ambiguous and imprecise. Image products (operational Experiment Data Record, EDRs) have sequential identifiers that are assigned on the ground (non-video images have unique identifiers). However, each EDR is associated with the specific telemetry data product from which it was created, and that source has an identifier (CDPID) assigned sequentially at the moment of acquisition. CDPID was extracted for every video thumbnail and downlinked image to provide the sequence of events for each transit.

The second challenge was to understand the time of each image. For each transit, all video thumbnails were assigned a most likely time, individually. This was taken to be SCLK (*i.e.*, truncated to whole second) plus 0.5 seconds, plus half of the exposure time. A fit of product ID to time then produced a linear relationship with residuals <0.5 s; the fit times were used. A reference time was established at the whole SCLK nearest the predicted event center, and this time was correlated to UTC. Time correlation (SCLK/UTC) was performed immediately after the transits, and drifts much less than that for Spirit or Opportunity [*c.f.*, ref. 1].

Finally, position was measured in each M-100 image (M-34 is omitted at this time) using triaxial ellipsoids and the JPL ephemeris for MSL-moon and MSL Sun distances. Typical results are shown in Fig. 3, with a red outline around the model satellite.

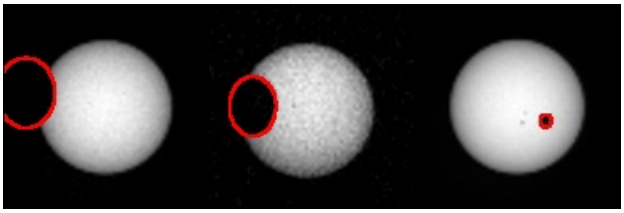

Fig. 3. Illustration of satellite model for sol 37, sol 42 Phobos, and sol 42 Deimos (left to right).

The JPL ephemeris was used as a baseline against which to measure position (Fig. 4). The Phobos closest approaches were closer (37) and farther (42) than predicted, and Deimos was farther—Δp in table 1. Phobos arrived on time, while Deimos was 3.0 sec early (Δt in table 1). In Table 1, Δx and Δy are the measured along-track (positive forward) and cross-track (positive North) position errors with respect to the JPL ephemeris. Each observed path was north of the ephemeris, by ~3.3 km for Phobos and 1.7 km for Deimos.

Uncertainties are still being evaluated, particularly systematic errors related to time and rover position (drives since landing are accounted for). The time error is likely significant for Deimos and not so for Phobos. The cross-track errors amount to 1.4 pixels for Deimos and ~7 pixels for Phobos, and are likely significant.

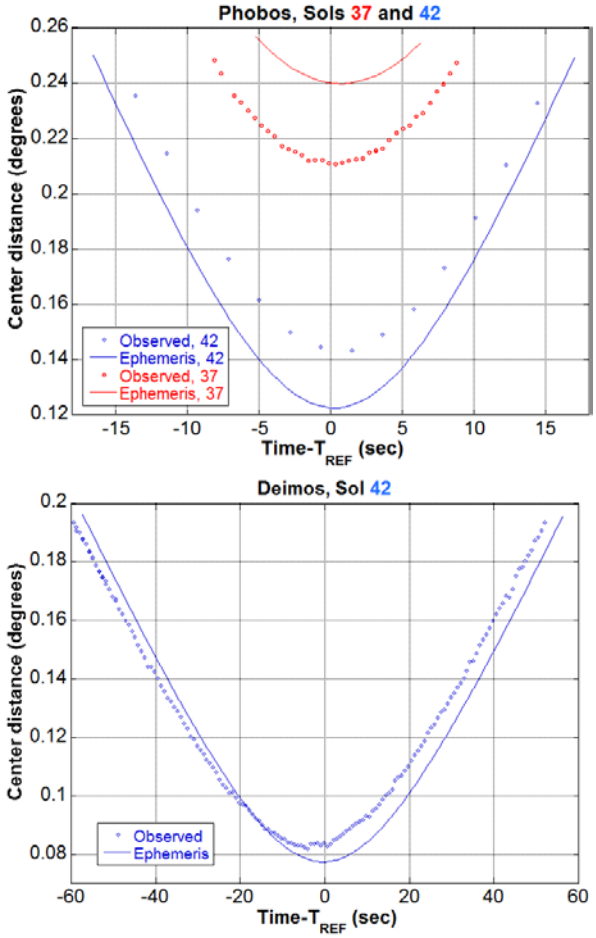

Fig. 4. Sun-Phobos and Sun-Deimos distance over time for observations (dots) and JPL ephemeris (line) for sol 37 (red) and 42 (blue).

Acknowledgments: T. Duxbury provided valuable assistance in observation planning.

References: [1] Bell, J.F., *et al.* (2005) *Nature* **436**, 55-57. [2] Bills, B.G., *et al.* (2005) *J.Geophys.Res.* **E07004**. [3] Lainey, V., *et al.* (2007) *Astron&Astrophys* **465** 1075-1084. [4] Barderas, G., *et al.* (2012) *MNRAS* **426**, 3195-3200.